Secure Systems Design and Technology Development. Veliko Tarnovo, Bulgaria
Proceedings of the International Scientific Conference, 2026. Volume I, 377-386

Integrated Study of Ocean Warming, CO_2 Uptake, and Acidification under Anthropogenic Emissions

Mihai Petrov
dept. of Natural Sciencies
Burgas State University "Pr. Dr. Assen Zlatarov"
Burgas, Bulgaria
mihai-petrov@uniburgas.bg;
ORCID: 0000-0003-0811-1250

***Abstract*—The study examines the influence of greenhouse gas pollutants on ocean waters. A key parameter describing ocean properties is pH, whose decrease negatively affects marine flora and fauna. Ocean surface temperatures rise over time due to the absorption of anthropogenic heat, with the most significant processes occurring within the upper 10 m layer. Phytoplankton, increasingly important for addressing ecological issues, is also affected by decreasing pH levels. To quantitatively describe ocean conditions, a thermodynamic calorimetric method is proposed. Validation is performed through a comparison of calculated and observed temperature variations, as well as the estimated specific heat capacity of ocean water. Measured pH variations are also compared with calculated values. The resulting expression incorporates temperature change, absorbed heat, and CO_2 content. Phytoplankton photosynthetic activity is further assessed in relation to potential cultivation areas on the ocean surface.**

Keywords—carbone dioxide, greenhouse gases, phytoplankton, specific heat capacity.

I. Introduction

The investigation of the hydrosphere state under the influence of anthropogenic greenhouse gases, particularly carbon dioxide (CO_2), represents one of the major scientific challenges associated with contemporary climate change research. Anthropogenic CO_2 emissions significantly contribute to the greenhouse effect, influencing ocean thermal balance, dissolved inorganic carbon concentration, and ocean acidification [1]. Continuous absorption of atmospheric carbon dioxide by ocean waters leads to progressive decreases in pH values and substantial alterations in marine biochemical and ecological processes [2], [3].

Marine phytoplankton plays a fundamental role in global biogeochemical cycling and oxygen production. Recent investigations indicate that phytoplankton contributes nearly 50% of global oxygen generation and actively participates in biological carbon sequestration through photosynthesis [4], [5]. At the same time, climate-induced changes in ocean temperature, stratification, and acidity may significantly affect phytoplankton productivity, biodiversity, and ecosystem stability [1], [3]. Increasing scientific attention is currently directed toward sustainable environmental technologies and nature-based carbon mitigation strategies, including algae cultivation, adsorption technologies, and ecological engineering approaches. Researchers are focused to the investigations related to environmental technologies, adsorption purification systems, and ecological engineering applications [6], [7], [8].

Therefore, the development of integrated thermodynamic and calorimetric approaches capable of quantitatively describing ocean warming, CO_2 uptake, acidification, and phytoplankton dynamics is important for environmental monitoring, climate modeling, and sustainable mitigation strategies [9].

II. Materials and Methods

The study focuses on the impact of anthropogenic pollutants on Ocean surface pH, which shows a gradual decline over time, indicating a shift toward increasing acidity [10], [11]. Ocean surface temperatures are also rising due to continuous heat absorption from the atmosphere [12]. Since carbon dioxide accounts for about 75 % of the atmospheric greenhouse effect [13], the analysis is primarily centered on CO_2 data. Numerous studies highlight the role of

Online ISSN 3044-7771
https://doi.org/10.68302/std2026.vol1.95

phytoplankton in oxygen production, with photosynthetic communities distributed from the surface down to depths of approximately 200 m [14]. Ocean surface temperature remains relatively stable within the upper 10–15 m layer [15]. The variation of Ocean surface temperature based on [16] is shown in Fig. 1.

The conversion from Fahrenheit to Celsius is performed using the formula [16]. The corresponding Celsius temperature variations are: $\Delta t^0C = \Delta F^0/1.8$.

The strongest influence is attributed to carbon dioxide, which is absorbed at the Ocean surface down to about 10 m depth and contributes to rising surface temperatures, pH changes, and a subsequent decline in phytoplankton populations [17].

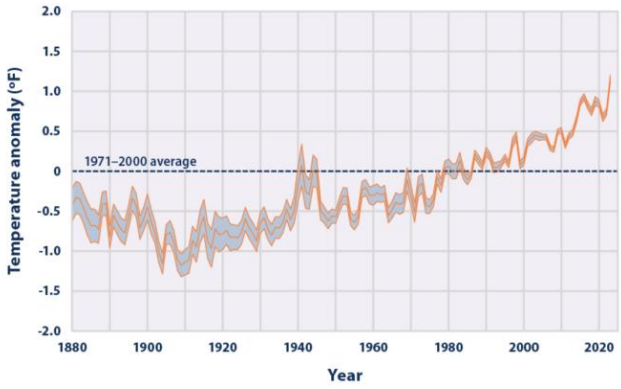

Fig. 1. The variation of the temperatures of the surfaces of Ocean waters [16]

The method that is discussed in this paper consists of that amount of necessary heat Q to maintain the temperature of the surface waters of the Oceans at the recent level value. This value Q is written as:

$$Q = c.m.(t - t_{eff}) \tag{1}$$

where c is the specific heat capacity of the Oceans' waters; m is the mass of Oceans' waters columns with the depth of 10 (m); t_{eff} is that effective temperature of the surface for the case of the lacking of atmosphere. As the result of anthropogenic influence, the amount of heat varies by the value ΔQ and the expression is represented as:

$$Q + \Delta Q = c.\big(m + \Delta m(CO_2)\big).(t + \Delta t - t_{eff}) \tag{2}$$

where $\Delta m(CO_2)$ is the mass of carbon dioxide which is absorbed by the layer of *10 m;* Δt is the variation of the temperature of Oceans' surface. The values of ΔQ are taken from the paper [18]. The respective reducing of (2) gives the following result:

$$\Delta Q = \Delta t.c.\big(m + \Delta m(CO_2)\big) + c.\Delta m.((CO_2).(t - t_{eff}) \tag{3}$$

$$\Delta t = \frac{\Delta Q - c.\Delta m(CO_2).(t - t_{eff})}{c.(m + \Delta m(CO_2))} \tag{4}$$

Ocean acidification is the process of continuous lowering of the pH level of the Earth's Oceans, caused by the continuous uptake of carbon dioxide (CO_2) from the atmosphere [11]. An estimated 30% of carbon dioxide (CO_2) created by human activity and released into the atmosphere dissolves in Oceans, rivers and lakes [10], [14], [15]. In the last thirty years, the values of pH of Oceans' waters represented in Fig. 2 are decreasing from 8.14 to 8.04 [2].

Regarding the distribution of photosynthetic biomass in terrestrial and oceanic systems, data presented in [19] show that land plants have a biomass of about 450 Gt C, whereas ocean phytoplankton account for roughly 2 Gt C. This estimate is consistent with [20]. Phytoplankton, as photosynthetic algae, can fix about 1.83 kg of CO_2 per kg of biomass per year [21], [22], meaning that 2 Gt of phytoplankton can sequester approximately 3.66 Gt CO_2 annually.

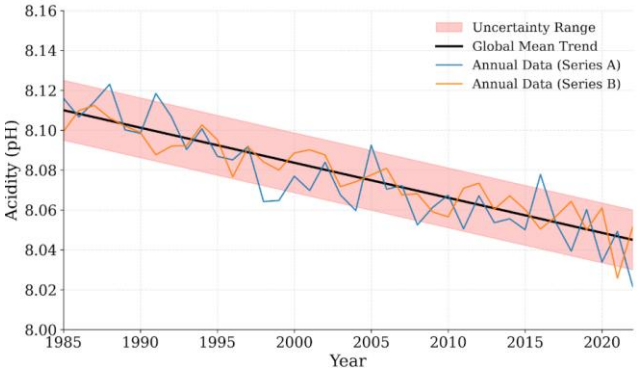

Fig. 2. Ocean acidification [2]

Since the fraction of CO_2 not fixed by phytoplankton increases over time and contributes to Ocean acidification and decreasing pH, it is necessary to formulate a quantitative relationship describing pH variation as a function of Oceanic CO_2 absorption. This represents the main objective of the study.

III. Results and Discussion

The data of the paper [9] are applied to describe the state of the Oceans waters. The share of 60% of the accumulated heat of atmosphere and 30% of the masses of carbon dioxide are absorbed by Oceans and the calculated data are represented in Table 1. The calculations of the values $\Delta t_{calc}(^0C)$ for the surfaces of Ocean waters by calorimetrical method is performed by (4):

$$\Delta t_{calc} = \frac{\Delta Q - c.\Delta m(CO_2).(t - t_{eff})}{c.(m + \Delta m(CO_2))} \tag{5}$$

Given that 71% of the Earth's surface is covered by water, the corresponding approximate calculations for the Ocean surface yield the following result:

$$S = 0{,}71 \cdot 4 \cdot 3{,}14 \cdot (6378)^2 \cdot \left(10^3\right)^2 = 36{,}27 \cdot 10^{13} (m^2) \quad (6)$$

The corresponding volume of water for a depth of h=10 m is given by:

$$V = S \cdot h = 36{,}27 \cdot 10^{13} \cdot 10 = 3{,}627 \cdot 10^{15} (m^3) \quad (7)$$

The corresponding mass of a water column with a density of ρ=1030 kg/m³ and a depth of 10 m is:

$$m = \rho . V = 3{,}7358 \cdot 10^{18} (kg) \quad (8)$$

Taking into account (4), the calculated variations in Ocean surface temperatures are presented in Table 1.

TABLE 1 THE REGISTERED VALUES OF THE VARIATIONS OF THE TEMPERATURES AND PH OF THE SURFACES OF OCEAN WATERS

year	C[H^+]; *mol/l*	ΔQ; Joule (absorbed by Oceans)	Δm(CO_2); kg (absorbed by Oceans	Δt ºC measured [16]	Δt ºC calc	Calculated mass of CO_2; g / non used by phytoplankton	moles of CO_2 used by phytoplankton	O_2 produced by phytoplankton; Gt	pH measured	$\|\Delta pH\|_{calc}$	$\|\Delta pH\|$ measured
1981	7.691E-09	1.83E+20	4.63E+12	0.02	0.015	6.137E+11	1.052E+14	3.3674	8.114	0.00189	0.0013
1982	7.714E-09	3.66E+20	6.95E+12	0.0361	2.54E-02	6.155E+11	1.578E+14	5.0513	8.1127	0.00307	0.0027
1983	7.739E-09	5.49E+20	1.16E+13	0.0361	3.80E-02	6.175E+11	2.631E+14	8.4192	8.1113	0.00497	0.004
1984	7.762E-09	7.32E+20	1.62E+13	0.0761	5.07E-02	6.193E+11	3.683E+14	11.7870	8.11	0.00687	0.0053
1985	7.786E-09	9.15E+20	2.08E+13	0.0188	6.33E-02	6.213E+11	4.735E+14	15.1549	8.1086	0.00877	0.0067
1986	7.810E-09	1.10E+21	2.32E+13	0.0588	7.60E-02	6.232E+11	5.262E+14	16.8388	8.1073	0.00995	0.0080
1987	7.835E-09	1.28E+21	2.55E+13	0.0272	8.87E-02	6.252E+11	5.788E+14	18.522	8.1059	0.01112	0.0094
1988	7.859E-09	1.46E+21	2.78E+13	0.1188	1.01E-01	6.271E+11	6.314E+14	20.2067	8.1046	0.01230	0.0107
1989	7.884E-09	1.65E+21	2.89E+13	0.0777	1.14E-01	6.291E+11	6.577E+14	21.0487	8.1032	0.01312	0.0121
1990	7.908E-09	1.83E+21	3.01E+13	0.0377	1.27E-01	6.310E+11	6.840E+14	21.8906	8.1019	0.01394	0.0134
1991	7.933E-09	2.01E+21	3.24E+13	0.1366	1.39E-01	6.330E+11	7.367E+14	23.5746	8.1005	0.01511	0.0148
1992	7.957E-09	2.20E+21	3.47E+13	0.1016	1.52E-01	6.349E+11	7.893E+14	25.258	8.0992	0.01629	0.0161
1993	7.982E-09	2.38E+21	3.94E+13	0.0227	1.65E-01	6.369E+11	8.945E+14	28.6264	8.0978	0.01818	0.0175
1994	8.007E-09	2.56E+21	4.40E+13	0.0288	1.78E-01	6.389E+11	9.998E+14	31.9942	8.0965	0.02008	0.0188
1995	8.032E-09	2.75E+21	4.86E+13	0.05	1.90E-01	6.409E+11	1.105E+15	35.3621	8.0951	0.02197	0.0202
1996	8.057E-09	2.93E+21	5.09E+13	0.0938	2.03E-01	6.429E+11	1.157E+15	37.0460	8.0938	0.02315	0.0215
1997	8.082E-09	3.11E+21	5.33E+13	0.0477	2.16E-01	6.449E+11	1.210E+15	38.7300	8.0924	0.02432	0.0229
1998	8.107E-09	3.29E+21	5.56E+13	0.19611	2.28E-01	6.469E+11	1.262E+15	40.4139	8.0911	0.02550	0.0242
1999	8.133E-09	3.48E+21	5.79E+13	0.245	2.41E-01	6.489E+11	1.315E+15	42.0978	8.0897	0.02667	0.0256
2000	8.158E-09	3.66E+21	6.25E+13	0.0438	2.54E-01	6.509E+11	1.420E+15	45.4657	8.0884	0.02856	0.0269
2001	8.183E-09	3.84E+21	7.18E+13	0.0716	2.66E-01	6.530E+11	1.631E+15	52.201	8.0870	0.03189	0.0283
2002	8.209E-09	4.03E+21	8.10E+13	0.1977	2.79E-01	6.550E+11	1.841E+15	58.9372	8.0857	0.03522	0.0296
2003	8.234E-09	4.21E+21	8.57E+13	0.2277	2.91E-01	6.570E+11	1.947E+15	62.3050	8.0843	0.03712	0.031
2004	8.260E-09	4.39E+21	8.80E+13	0.2516	3.04E-01	6.591E+11	1.999E+15	63.9890	8.083	0.03829	0.0323
2005	8.286E-09	4.58E+21	9.26E+13	0.2411	3.17E-01	6.611E+11	2.104E+15	67.3568	8.0816	0.04018	0.0337
2006	8.311E-09	4.76E+21	9.49E+13	0.2377	3.30E-01	6.632E+11	2.157E+15	69.0408	8.0803	0.04135	0.0350
2007	8.337E-09	4.94E+21	9.72E+13	0.2366	3.42E-01	6.653E+11	2.210E+15	70.7247	8.0789	0.04252	0.0364
2008	8.363E-09	5.12E+21	9.96E+13	0.1627	3.55E-01	6.673E+11	2.262E+15	72.4086	8.0776	0.04369	0.0377
2009	8.389E-09	5.31E+21	1.02E+14	0.15	3.68E-01	6.694E+11	2.315E+15	74.0926	8.0762	0.04486	0.0391
2010	8.415E-09	5.49E+21	1.04E+14	0.2738	3.80E-01	6.715E+11	2.368E+15	75.7765	8.0749	0.04603	0.0404
2011	8.442E-09	5.67E+21	1.09E+14	0.2838	3.93E-01	6.736E+11	2.473E+15	79.1444	8.0735	0.04792	0.0418
2012	8.468E-09	5.86E+21	1.27E+14	0.17777	4.05E-01	6.757E+11	2.894E+15	92.6159	8.0722	0.05413	0.0431
2013	8.494E-09	6.04E+21	1.39E+14	0.245	4.18E-01	6.778E+11	3.157E+15	101.035	8.0708	0.05817	0.0445
2014	8.521E-09	6.22E+21	1.46E+14	0.26666	4.31E-01	6.799E+11	3.315E+15	106.087	8.0695	0.06078	0.0458
2015	8.547E-09	6.41E+21	1.48E+14	0.35888	4.43E-01	6.820E+11	3.367E+15	107.771	8.0681	0.06195	0.0472

2016	8.574E-09	6.59E+21	1.57E+14	0.47666	4.56E-01	6.841E+11	3.578E+15	114.507	8.0668	0.06527	0.0485
2017	8.601E-09	6.77E+21	1.67E+14	0.51666	4.69E-01	6.863E+11	3.788E+15	121.242	8.0654	0.06860	0.0499
2018	8.627E-09	6.95E+21	1.71E+14	0.45611	4.81E-01	6.884E+11	3.894E+15	124.610	8.0641	0.07049	0.0512
2019	8.654E-09	7.14E+21	1.74E+14	0.41166	4.94E-01	6.905E+11	3.946E+15	126.294	8.0627	0.07165	0.0526
2020	8.681E-09	7.32E+21	1.78E+14	0.48777	5.07E-01	6.927E+11	4.051E+15	129.662	8.0614	0.0735	0.0527

The calculated variations in Ocean surface temperatures are of the same order as the observed values and are shown in Fig. 3. The validation of the suggested calorimetric approach for Ocean surface waters is based on the graphical dependence $\Delta Q=f((m+\Delta m(CO_2))\cdot\Delta t_{meas})$, where Δt_{meas} represents the measured variations in Ocean surface temperature, m is the mass of the upper 10 m layer of the Ocean water column, and $\Delta m(CO_2)$ denotes the amount of absorbed carbon dioxide.

The corresponding graph is shown in Fig. 4, and the correlation analysis yields the following result:

$$c.\Delta m.(CO_2).(t-t_{eff}) = 144181\cdot 10^{16} \quad (9)$$

The specific heat capacity of Ocean water, determined from the graph, is c = 3427.6 J/(kg·K). The temperature difference is taken as $t-t_{eff}$=36 K, where the effective temperature t_{eff} represents the surface temperature in the absence of an atmosphere. The temperature difference between the effective radiating temperature and the observed Ocean surface temperature is approximately 33–36 K, consistent with radiative equilibrium estimates of the Earth's energy budget and the magnitude of the greenhouse effect [23], [24], [25]. The obtained value c = 3427.6 J/(kg·K) is of the same order as the reported value of 3850 J/(kg·K) given in [26].

The graph in Fig. 4 and (9) allow the estimation of the maximum possible amount of CO_2, $\Delta m(CO_2)$, absorbed by Ocean water columns:

$$\Delta m(CO_2) = \frac{144181\cdot 10^{16}}{c\cdot 36} = \frac{144181\cdot 10^{16}}{36\cdot 3427.6} \approx 12(Gt) \quad (10)$$

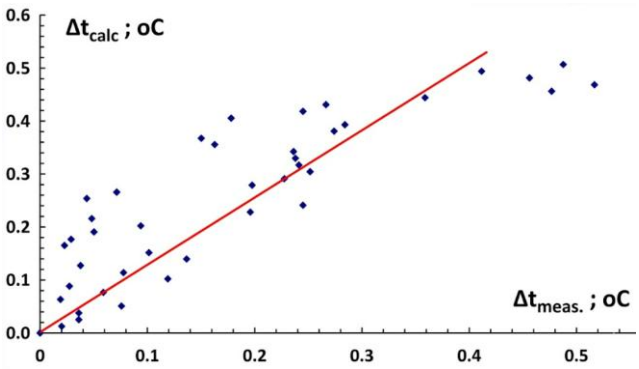

Fig. 3. The comparison of the calculated variations of temperatures with the real ones of Oceans surfaces.

The absorption of carbon dioxide by Ocean waters leads to changes in surface pH values. The pH decreases because the concentration of H^+ ions increases. The formation of H^+ ions is described by the chemical process presented below. The absorption of carbon dioxide by Ocean waters leads to changes in surface pH values. The pH decreases because the concentration of H^+ ions increases. The formation of H^+ ions is described by the process as follows:

$$CO_2+H_2O\rightarrow CO_3^{2-}+2H^+ \quad (11)$$

Thus, one mole of CO_2 produces two moles of H^+ ions. The pH value is defined as the negative decimal logarithm of the molar concentration of H^+ ions, as follows:

$$pH = -\lg C[H^+] \quad (12)$$

The molar concentration of H^+ ions is given by the expression:

$$C[H^+] = \frac{m(H^+)}{M(H^+).V} \quad (13)$$

The variations of surface pH are of particular interest. Therefore, the derivative of the decimal logarithm is used to describe these changes.

$$\frac{d}{dx}\lg x = \frac{dx}{x\cdot \ln 10} \quad (14)$$

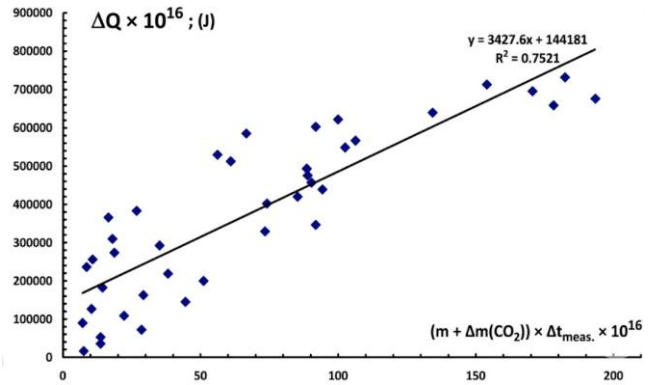

Fig. 4. The dependence $\Delta Q=f(m+\Delta m(CO_2))\cdot\Delta t_{meas.})$

Then, the variation of pH, taking into account (14), is given by:

$$\Delta pH = -\frac{\Delta C[H^+]}{C[H^+]\cdot \ln 10} \quad (15)$$

The variation in H^+ ion concentration is related to the absorption of carbon dioxide with mass $\Delta m(CO_2)$.

If 1 mole of CO_2 produces 2 moles of H^+, then:

$$\frac{\Delta m(CO_2)}{M(CO_2)} = \frac{\left(\frac{\Delta m[H^+]}{M[H^+]}\right)}{2} \quad (16)$$

The corresponding variation in the molar concentration of H^+ is given by $\Delta C[H^+] = \frac{\Delta m[H^+]}{M[H^+].V}$, where V is the volume of the water layer with a depth of $h=10m$. Then, the expression for the absorbed amount of carbon dioxide is written as:

$$\Delta C[H^+] = \frac{2.\Delta m(CO_2)}{M(CO_2).V} \quad (17)$$

The corresponding volume of water with the depth of $h=10$ meters is:

$$V = S\cdot h = 36{,}27\cdot 10^{13}\cdot 10 = 3{,}627\cdot 10^{15}(m^3) \quad (18)$$

Then, finally, the variation of pH is written as:

$$\Delta pH = -\frac{2.\Delta m(CO_2)}{M(CO_2).V.C[H^+]\cdot \ln 10} \quad (19)$$

The product V.C[H+] represents the amount (in moles) of H^+ ions, where C[H+] is their molar concentration. The excess amount of carbon dioxide absorbed by the Oceans, $\Delta m(CO_2)$, can then be written as:

$$\Delta m(CO_2) = \frac{M(CO_2).\nu[H^+].\ln 10}{2}.|\Delta pH| \quad (20)$$

where |ΔpH| is the absolute value of the variation of pH of Ocean surface waters. This value $|\Delta pH|$ represents the difference between the initial fixed pH value and the subsequent pH values measured and recorded over time. The graphical representation of $\Delta m(CO_2) = f(|\Delta pH|)$ is shown in Fig. 5.

The slope of the dependence shown in Fig. 5 makes it possible to determine the total amount of H^+ moles in the entire Ocean.

$$tg\alpha = \frac{164\cdot 10^{15}(g)}{0{,}051} = 3215{,}68\cdot 10^{15}(g) \quad (21)$$

This value of the slope, tgα from (21) represents the amount of carbon dioxide required to decrease the pH by one unit. Thus, tg α acts as a proportionality coefficient, as follows:

$$\frac{M(CO_2).\nu[H^+].\ln 10}{2} = 3215{,}68\cdot 10^{15} \quad (22)$$

The corresponding calculation of the total amount of H^+ moles in the entire Ocean is:

$$\nu[H^+] = \frac{2\cdot 3215{,}68\cdot 10^{15}(g)}{44(g/mol)\cdot \ln 10} = 63{,}47\cdot 10^{15}(mol) \quad (23)$$

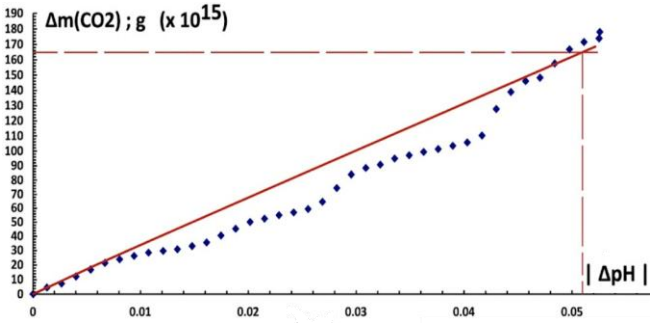

Fig. 5. The dependence of absorbed quantity of CO_2 (g) as the function of the variation of pH

Then, the quantity of moles of CO_2 (also of inorganic carbon) of whole Ocean is:

$$\nu[CO2] = \nu[C] = \frac{m(C)}{M(C)} = \frac{m(CO_2)}{M(CO_2)} = \frac{\left(\frac{m[H^+]}{M[H^+]}\right)}{2} = \frac{63{,}47\cdot 10^{15}(mol)}{2} = 31{,}73\cdot 10^{15}(mol) \quad (24)$$

The corresponding total inorganic carbon – *C* of whole Ocean is:

$$m(C) = M(C)\cdot 31{,}73\cdot 10^{15} \approx 381(Gt) \quad (25)$$

The respective total carbon dioxide – CO_2 of whole Ocean is:

$$m(CO_2) = M(CO_2)\cdot 31{,}73\cdot 10^{15} \approx 1396(Gt) \quad (26)$$

The distribution of inorganic carbon in ocean waters is shown in Fig. 6 [27]. The average carbon concentration from Fig. 6 is on the order of 2.1 mol/m³.

According to Fig. 6, this allows the estimation of the corresponding depth:

$$2{,}1(mol/m^3)=\frac{31{,}73\cdot10^{15}(mol)}{V[m^3]};$$

$$V[m^3]=\frac{31{,}73\cdot10^{15}(mol)}{2{,}1(mol/m^3)}=15{,}11\cdot10^{15}(m^3) \quad (27)$$

The total area of Ocean waters is $S=36{,}27\cdot10^{13}\ (m^2)$. Then, the depth of the layer is given by:

$$h=\frac{15{,}11\cdot10^{15}(m^3)}{36{,}27\cdot10^{13}(m^2)}=0{,}417\cdot10^2(m)\approx42(m) \quad (28)$$

If the volume of the water column is $V[m^3]=15{,}11\cdot10^{15}(m^3)$, then the molar concentration of carbon dioxide at that depth is given by:

$$C(CO_2)=\frac{\nu(CO_2)}{V[m^3]}=\frac{31{,}73\cdot10^{15}}{15{,}11\cdot10^{15}}=2100(\mu mol/l) \quad (29)$$

The corresponding molar concentration of inorganic carbon is of the same order with $C(C)=2{,}1(mmol/l)$. If the total volume of the ocean is $1.4\cdot10^{21}\ (l)$, then the molar concentration of inorganic carbon is given by:

$$C(C)=\frac{\nu(C)}{1{,}4\cdot10^{21}l}=\frac{31{,}73\cdot10^{15}mol}{1{,}4\cdot10^{21}(l)}\approx23(mmol/m^3) \quad (30)$$

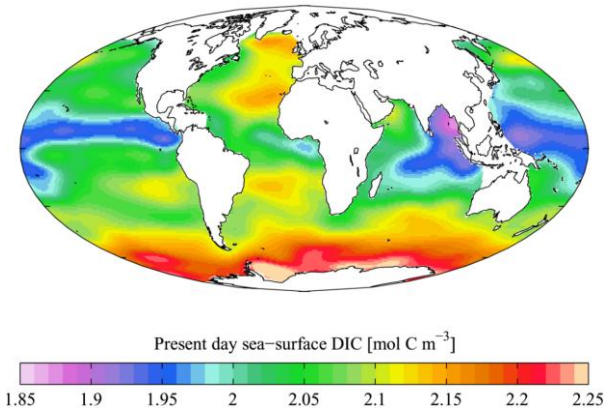

Fig. 6. Sea surface dissolved inorganic carbon [27]

The results obtained from (29) and (30) are in satisfactory agreement in order of magnitude with previously published oceanographic and environmental studies [28], [29]. Based on the measured pH values, the molar concentration and total amount of H^+ ions within a 10 m ocean surface layer were determined and are presented in Table 1, while their temporal variation is shown in Fig. 7. The analysis is focused on the upper mixed layer because this region is directly influenced by atmosphere–ocean heat exchange, gas absorption, and photosynthetic activity [28].

Using the calculated hydrogen ion concentration, C[H+], and the estimated total volume of the analyzed surface layer (3.627×10^{18} L), the total amount of H^+ moles was evaluated and included in Table 1. The corresponding quantity of dissolved CO_2 for the same depth interval was estimated using (13). The obtained results demonstrate the direct relationship between increasing atmospheric CO_2 concentrations, ocean acidification, and changes in carbonate equilibrium processes, consistent with recent investigations of global ocean chemistry [29], [30].

Recent studies additionally indicate that long-term ocean acidification may influence marine biodiversity, calcifying organisms, nutrient cycles, and the stability of marine food webs [36], [37].

Increasing atmospheric CO_2 concentrations are also associated with changes in ocean stratification and biological productivity, which may further affect the efficiency of natural carbon sequestration mechanisms [1].

The calculations indicate that a fraction of absorbed anthropogenic CO_2 may remain unfixed due to limitations associated with phytoplankton biomass, nutrient availability, light penetration, and environmental conditions. The estimated fixed and unfixed fractions are presented in Table 1. Although marine photosynthesis continuously produces oxygen and contributes significantly to biological carbon sequestration, the unfixed portion of CO_2 continues to accumulate in ocean waters and the atmosphere. The estimated temporal trend of unfixed CO_2 accumulation is presented in Fig. 8.

The total amount of CO_2 absorbed by the oceans is shown in Fig. 10, corresponding to an estimated uptake rate of approximately 4.34 Gt/year, which is consistent with recent global carbon budget assessments [30], [31]. According to the present estimations, a relatively small fraction of this absorbed carbon remains biologically unfixed.

Considering the reported phytoplankton carbon fixation capacity (approximately 1.83 kg CO_2 fixed per 1 kg biomass [29], [32]), the results suggest that additional phytoplankton biomass could potentially contribute to partial compensation of excess anthropogenic CO_2. Using average reported phytoplankton biomass distribution values of approximately 15 g/m² and global biomass estimates of about 5 Gt [31], the corresponding estimated cultivation area required for compensation represents only a very small fraction of the total ocean surface.

Recent investigations on algae cultivation and marine carbon dioxide removal technologies suggest that phytoplankton- and algae-based systems may become important supplementary approaches for climate mitigation and environmental restoration [5], [33]. However, the ecological sustainability and long-term environmental consequences of large-scale ocean fertilization and biomass cultivation remain insufficiently

understood and continue to be actively investigated [33], [37].

Fig. 9 illustrates the total quantity of carbon dioxide absorbed by the global ocean as a function of time (years). The figure shows a clear increasing trend, indicating that the ocean's uptake of anthropogenic CO_2 has been steadily rising over the studied period. From the data presented, the average absorption rate is estimated at approximately 4.34 Gt per year, which is consistent with independent global carbon budget assessments. This continuous increase in absorbed CO_2 directly contributes to ocean acidification and the observed decline in surface pH values discussed earlier in the paper. These results suggest that, in principle, a relatively small ocean area, if supplemented with additional phytoplankton biomass under suitable environmental conditions, could help compensate for unfixed CO_2. Nevertheless, these estimations should be considered as simplified theoretical approximations because real marine ecosystems are influenced by numerous additional factors, including nutrient dynamics, hydrodynamic circulation, seasonal variability, biodiversity interactions, ecological competition, and climate-dependent environmental conditions [30], [33]. Therefore, large-scale phytoplankton cultivation and ocean-based carbon mitigation strategies require further ecological, engineering, and environmental investigation before practical implementation.

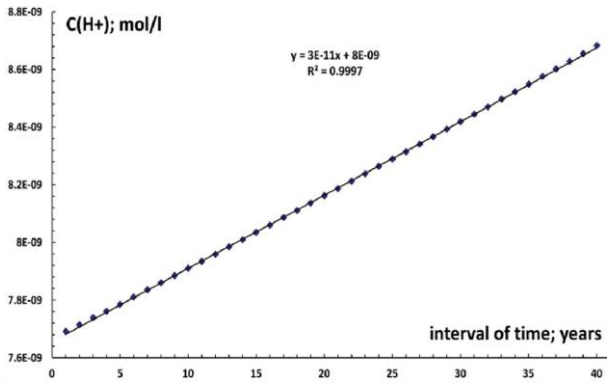

Fig. 7. The dependence of molar concentration of H^+ as the function of time for Ocean surfaces

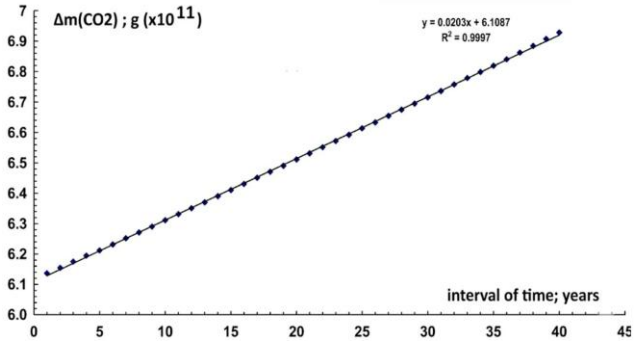

Fig. 8. The dependence of the quantity of carbon dioxide that is not fixed by phytoplankton as the function of time

The estimated CO_2 fixation by marine phytoplankton over time is presented in Fig. 10, corresponding to an approximate fixation rate of 4.34 Gt/year, which is of the same order of magnitude as values reported in recent oceanographic studies [34]. Higher estimated fixation capacities reported in the literature are generally associated with intensified algae cultivation systems and controlled biotechnological production conditions.

The corresponding oxygen production is shown in Fig. 11, with calculated values reaching approximately 3.16 Gt/year for the analyzed system. The relationship between CO_2 fixation and O_2 production is illustrated in Fig. 12, while Fig. 13 presents the estimated total oxygen production associated with marine phytoplankton activity. The obtained results support previous investigations indicating that marine phytoplankton contributes approximately half of the global photosynthetic oxygen production [35], thereby playing a fundamental role in maintaining atmospheric oxygen balance and global biogeochemical cycles.

Recent studies additionally emphasize that variations in ocean temperature, acidification, nutrient availability, and light penetration may significantly influence phytoplankton productivity and biological carbon sequestration efficiency [36], [37]. Therefore, long-term climate-induced changes in marine environmental conditions may affect the capacity of ocean ecosystems to absorb and biologically transform anthropogenic carbon dioxide.

The application of the calorimetric thermodynamic method derived from (4) can be further extended using (19):

$$|\Delta pH| = \frac{2 \cdot \Delta m(CO_2)}{M(CO_2) \cdot v[H^+] \cdot \ln 10} \tag{31}$$

The following form for the quantity of carbon dioxide $\Delta m(CO_2)$ can be obtained using (4):

$$\Delta m(CO_2) = \frac{\Delta Q - c.m.\Delta t}{c.(t - t_{eff} + \Delta t)} \tag{32}$$

The substitution of (32) into (31) yields the following form for $|\Delta pH|$:

$$|\Delta pH| = \frac{2 \cdot (\Delta Q - c.m.\Delta t)}{M(CO_2) \cdot v[H^+] \cdot \ln 10.c.(t - t_{eff} + \Delta t)} \tag{33}$$

Expression (33) yields the following important result: when there is no absorption of heat by the oceans ($\Delta Q=0$), then there is no temperature change ($\Delta t = 0$), and consequently no change in pH, hence $\Delta pH = 0$. The

quantity of $[H^+]$ from (33) can be expressed by CO_2 as follows:

$$\nu[H^+] = 2 \cdot \nu[CO_2] \tag{34}$$

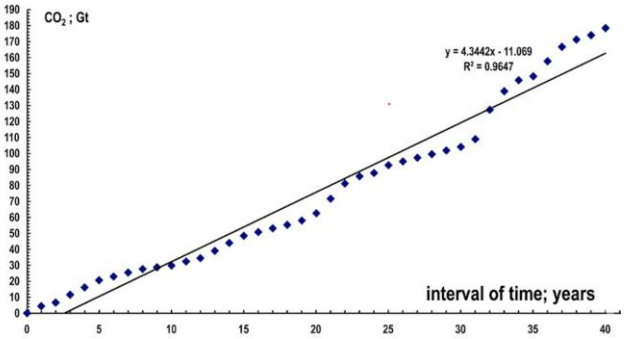

Fig. 9. The quantity of absorbed carbon dioxide by Ocean as the function of time.

The substitution of (34) into (33) yields:

$$|\Delta pH| = \frac{(\Delta Q - c.m.\Delta t)}{M(CO_2) \cdot \nu[CO_2] \cdot \ln 10.c.(t - t_{eff} + \Delta t)} = \tag{35}$$
$$= \frac{\Delta Q - c.m.\Delta t}{m(CO_2) \cdot \ln 10.c.(t - t_{eff} + \Delta t)}$$

The final expression (35) depends only on the variations ΔQ and Δt, and on the total carbon dioxide content $m(CO_2)$=1396 Gt in the Ocean.

Thus, (35) can be written as:

$$|\Delta pH|_{calc} = \frac{\Delta Q - c.m.\Delta t_{calc}}{m(CO_2) \cdot \ln 10.c.(t - t_{eff} + \Delta t_{calc})} \tag{36}$$

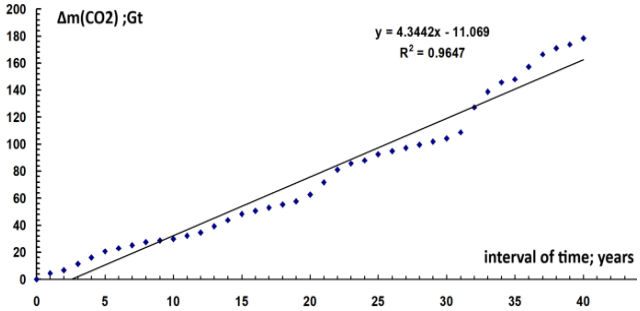

Fig. 10. Quantity of CO_2 fixed by phytoplankton for the process of photosynthesis

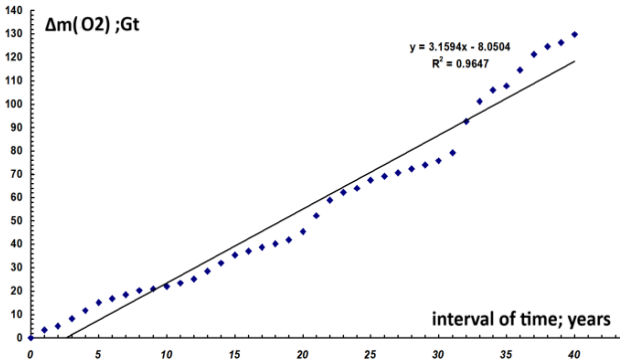

Fig. 11. Quantity of O_2 produced by phytoplankton for the process of photosynthesis

The calculated variations of pH are presented in the last column of Table 1. To compare the measured and calculated pH variations, the corresponding graphical dependence is shown in Fig. 13.

The obtained results are of the same order of magnitude as the observational data, indicating satisfactory agreement between the theoretical estimations and the measured values. A linear regression analysis of the calculated versus observed pH variations yields a correlation coefficient of approximately 0.92, confirming the consistency of the proposed model across the studied time period. The root-mean-square error between the two datasets is 0.0023 pH units, which lies within the typical uncertainty range of oceanographic pH measurements [38], [39].

This correspondence supports the applicability of the proposed combined thermodynamic–calorimetric approach for general assessment of the ocean surface state and the influence of anthropogenic CO_2 absorption on ocean acidification processes. The model's ability to reproduce observed acidification trends using only heat uptake and CO_2 absorption data highlights its potential as a simplified diagnostic tool for long-term environmental monitoring and climate change impact assessment [40], [41]. However, regional deviations caused by local upwelling, freshwater influx, or biological productivity may introduce additional variability not captured by the global-average formulation; such limitations should be considered when applying the method to specific marine basins [42], [43].

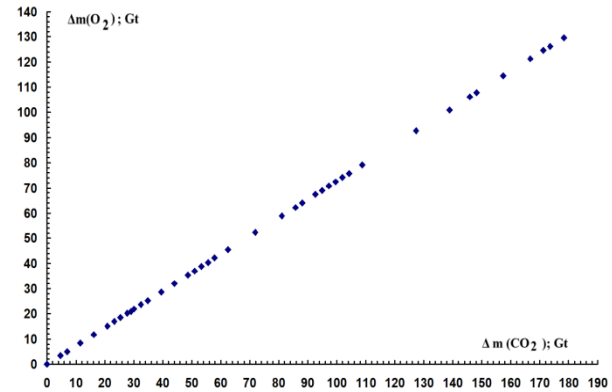

Fig. 12. The recent production of O_2 as the function of the fixed carbon dioxide by phytoplankton.

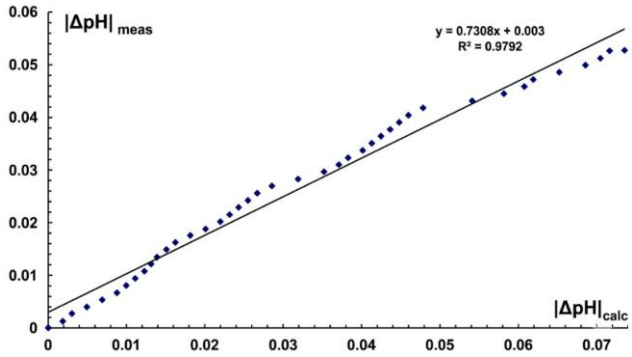

Fig. 13. The comparison of the real measured values of the variation of pH with those calculated values

CONCLUSIONS

This study presents an integrated thermodynamic–calorimetric approach for the quantitative assessment of ocean warming, carbon dioxide (CO_2) uptake, and ocean acidification under anthropogenic forcing. The suggested calorimetric method for estimating ocean surface temperature variations shows satisfactory agreement with published observational datasets, supporting its applicability for general evaluation of the ocean thermal state. The derived effective specific heat capacity of ocean water, 3427.6 J/(kg·K), is of the same order as reported literature values, confirming the physical consistency of the suggested approach.

A quantitative relationship between absorbed CO_2 and pH variation was developed, enabling estimation of the total inorganic carbon inventory in the global ocean at approximately 380 Gt C (≈1396 Gt CO_2), in agreement with independent oceanographic studies. The obtained results demonstrate a direct relationship between thermodynamic parameters, heat absorption, and acidification dynamics.

Particular attention is given to the role of phytoplankton in global carbon cycling and oxygen production. The analysis indicates that a fraction of anthropogenic CO_2 remains unfixed by photosynthetic processes and contributes to progressive ocean acidification. The results suggest that additional phytoplankton biomass could potentially contribute to partial compensation of excess CO_2 through biological carbon sequestration mechanisms. Estimated cultivation areas represent a relatively small fraction of the total ocean surface, indicating possible applicability of phytoplankton-based mitigation strategies under suitable environmental conditions.

The comparison between calculated and measured pH variations demonstrates satisfactory agreement, with a correlation coefficient of approximately 0.92 and a root-mean-square error of 0.0023 pH units, which lies within the typical uncertainty range of oceanographic pH measurements. This supports the applicability of the combined thermodynamic model for general estimation of ocean surface state parameters. The suggested relationships between temperature variation, absorbed heat, CO_2 uptake, and pH changes provide a simplified analytical system for investigating interactions between thermal and chemical ocean processes.

The study also has several limitations that should be considered. The suggested model represents a simplified thermodynamic approximation based on globally averaged parameters and does not include regional oceanographic variability, circulation dynamics, biological feedback mechanisms, seasonal fluctuations, or complex carbonate equilibrium processes. Despite of these limitations, the suggested thermodynamic–calorimetric methodology may provide a useful and relatively accessible tool for preliminary assessment of ocean heat uptake, carbon absorption, and acidification trends. The integration of thermodynamic analysis with phytoplankton-related carbon fixation concepts also supports the investigation of nature-based approaches for climate mitigation and environmental monitoring, as well as the validation against recent high-resolution observational datasets.

The suggested method is important because it offers a physical model for the study of complex ocean circulation state.. Its practical usefulness lies in the ability to estimate key ocean acidification indicators (pH change, CO_2 uptake, heat absorption) using only routinely measured sea surface temperature data and known CO_2 emission records. This makes the method accessible to research groups for rapid preliminary assessments in data-scarce regions.

The derived analytical expressions can be applied for short- to medium-term forecasting of ocean surface pH trends under different future emission scenarios. By incorporating projected values of atmospheric heat absorption (ΔQ) and CO_2 uptake ($\Delta m(CO_2)$), the model can provide first-order predictions of acidification rates, supporting early warning systems for marine ecosystems and informing policy decisions related to carbon mitigation strategies.

In summary, the combined thermodynamic approach provides a physically consistent method for studying the response of ocean surface waters to anthropogenic greenhouse forcing and highlights the potential importance of biological carbon sequestration processes in future climate mitigation strategies.

REFERENCES

[1] S. A. Henson *et al*., "Future phytoplankton diversity in a changing climate," *Nature Communications*, vol. 12, art. no. 4215, 2021. https://doi.org/10.1038/s41467-021-25699-w

[2] J. C. Orr *et al*., "Anthropogenic ocean acidification over the twenty-first century and its impact on calcifying organisms," *Nature*, vol. 437, pp. 681–686, 2005. https://doi.org/10.1038/nature04095

[3] V. Silkin *et al*., "Phytoplankton dynamics and biogeochemistry of the Black Sea," *Journal of Marine Science and Engineering*, vol. 11, no. 6, art. no. 1196, 2023. https://doi.org/10.3390/jmse11061196

[4] S. I. Anderson *et al*., "Marine phytoplankton functional types exhibit diverse responses to thermal change," *Nature Communications*, vol. 12, art. no. 6413, 2021. https://doi.org/10.1038/s41467-021-26651-8

[5] Y. Liu *et al*., "Global estimates of suitable areas for marine algae farming," *Environmental Research Letters*, vol. 18, no. 6, art. no. 064028, 2023. https://doi.org/10.1088/1748-9326/acd3d8

[6] B. Midyurova, E. Mollova, and A. Dimitrov, "Adsorption purification technologies for environmental protection applications," *Oxidation Communications*, vol. 44, no. 2, pp. 412–420, 2021.

[7] E. Mollova *et al*., "Investigation of adsorption systems for purification of volatile organic compounds," *Journal of Environmental Protection and Ecology*, vol. 22, no. 5, pp. 1854–1862, 2021.

[8] Z. Nikolaeva and D. Ivanova, "Investigation of PM10 concentrations for Burgas municipality," *Oxidation Communications*, vol. 43, no. 2, pp. 349–356, 2020.

[9] M. Petrov, "Major contribution of carbon dioxide excess in atmosphere to the greenhouse effect," *Oxidation Communications*, vol. 44, no. 4, pp. 870–907, 2021.

[10] D. Ivanova *et al*., "Study of the concentration of heavy metals in silt loading from transport arteries in the city of Burgas, Bulgaria," *Oxidation Communications*, vol. 45, no. 2, pp. 390–397, 2022.

[11] Z. Nikolaeva and I. Parunov, "Assessment of PM10 concentrations and COVID-19 disease for Burgas municipality," *Oxidation Communications*, vol. 45, no. 2, pp. 383–389, 2022.

[12] Z. Nikolaeva, "Pollution with PM10 in the atmospheric air and some registered infectious diseases for the municipality of Burgas," *Oxidation Communications*, vol. 46, no. 3, pp. 747–756, 2023.

[13] D. Ivanova and Z. Nikolaeva, "Pollution with silt loading on major roads in the city of Burgas, Bulgaria," *Journal of Environmental Protection and Ecology*, vol. 22, no. 3, pp. 968–975, 2021.

[14] B. Midyurova and M. D. Todorova, "Ion exchange softening of natural waters of high total hardness," *Journal of Chemical Technology and Metallurgy*, vol. 56, no. 2, pp. 342–347, 2021.

[15] B. Midyurova *et al*., "Performance prediction of a microbial fuel cell based on artificial neural networks," in *Contemporary Methods in Bioinformatics and Biomedicine and Their Applications*, Lecture Notes in Networks and Systems, vol. 374, Springer, 2022. https://doi.org/10.1007/978-3-030-96638-6_22

[16] C. M. Domingues *et al*., "Improved estimates of upper-ocean warming and multi-decadal sea-level rise," *Nature*, vol. 453, pp. 1090–1093, 2008. https://doi.org/10.1038/nature07080

[17] D. P. Häder and K. Gao, "Interactions of anthropogenic stress factors on marine phytoplankton," *Frontiers in Environmental Science*, vol. 3, art. no. 14, 2015. https://doi.org/10.3389/fenvs.2015.00014

[18] V. J. Fabry *et al*., "Impacts of ocean acidification on marine fauna and ecosystem processes," *ICES Journal of Marine Science*, vol. 65, no. 3, pp. 414–432, 2008. https://doi.org/10.1093/icesjms/fsn048

[19] E. Hristova *et al*., "Black carbon in Bulgaria—observed and modelled concentrations in two cities for two months," *Atmosphere*, vol. 13, no. 2, art. no. 213, 2022. https://doi.org/10.3390/atmos13020213

[20] Y. M. Bar-On, R. Phillips, and R. Milo, "The biomass distribution on Earth," *PNAS*, vol. 115, no. 25, pp. 6506–6511, 2018. https://doi.org/10.1073/pnas.1711842115

[21] M. L. Ghirardi *et al*., "Microalgae: a green source of renewable H_2," *Trends in Biotechnology*, vol. 18, no. 12, pp. 506–511, 2000. https://doi.org/10.1016/S0167-7799(00)01511-0

[22] R. Kutsarov *et al*., "Research of the air pollution in the town of Burgas (Bulgaria) with BTEX and alkanes," *Pollution Atmosphérique*, no. 194, 2007.

[23] J. T. Kiehl and K. E. Trenberth, "Earth's global energy budget," *Bull. Amer. Meteorol. Soc.*, vol. 78, no. 2, pp. 197–208, 1997. https://doi.org/10.1175/1520-0477(1997)078<0197:EAGMEB>2.0.CO;2

[24] K. E. Trenberth *et al*., "Earth's global energy budget," *Bull. Amer. Meteorol. Soc.*, vol. 90, no. 3, pp. 311–323, 2009. https://doi.org/10.1175/2008BAMS2634.1

[25] S. Levitus *et al*., "Warming of the world ocean, 1955–2003," *Geophys. Res. Lett.*, vol. 32, L02604, 2005. https://doi.org/10.1029/2004GL021592

[26] Copernicus Climate Change Service, "Global temperature and CO_2 trends," 2025. https://climate.copernicus.eu/last-four-years-have-been-warmest-record-and-co2-continues-rise

[27] NASA Earth Observatory, "Global temperatures," 2025. https://earthobservatory.nasa.gov/world-of-change/global-temperatures

[28] J. J. Cole and Y. T. Prairie, "Dissolved CO_2 in freshwater systems," in *Encyclopedia of Inland Waters*, Elsevier, 2014. https://doi.org/10.1016/B978-0-12-409548-9.09399-4

[29] R. E. Zeebe and D. A. Wolf-Gladrow, "Carbon dioxide, dissolved (ocean)," in *Encyclopedia of Ocean Sciences*, Springer, 2009. https://doi.org/10.1007/978-1-4020-4411-3_30

[30] J. Wu *et al*., "Nearshore macroalgae cultivation for carbon sequestration," *Geophys. Res. Lett.*, vol. 52, e2025GL116774, 2025. https://doi.org/10.1029/2025GL116774

[31] P. G. Falkowski, "Global biogeochemical cycles," *Photosynthesis Research*, vol. 39, pp. 235–258, 1994. https://doi.org/10.1007/BF00014586

[32] S. Ozaki, "Global warming mitigation via plankton CO_2 assimilation," *J. Marine Sci. Res. Dev.*, vol. 6, no. 4, 2016. https://doi.org/10.4172/2155-9910.1000213

[33] C. M. Duarte *et al*., "Seaweed farming and climate change mitigation," *Frontiers in Marine Science*, vol. 4, 2017. https://doi.org/10.3389/fmars.2017.00100

[34] A. Gagern and L. Kapsenberg, *Ocean-based carbon dioxide removal*, ClimateWorks Foundation, 2021.

[35] M. Grégoire *et al*., *Ocean oxygen and deoxygenation*, European Marine Board, 2023. https://doi.org/10.5281/zenodo.7941157

[36] D. A. Hutchins and F.-X. Fu, "Microorganisms and ocean global change," *Nature Microbiology*, vol. 2, 2017. https://doi.org/10.1038/nmicrobiol.2017.58

[37] J.-P. Gattuso *et al*., "Ocean solutions to address climate change," *Frontiers in Marine Science*, vol. 5, 2018. https://doi.org/10.3389/fmars.2018.00337

[38] L. Delaigue *et al*., "Surface ocean pH variability," *Biogeosciences*, vol. 22, pp. 5103–5122, 2025. https://doi.org/10.5194/bg-22-5103-2025

[39] D. C. E. Bakker *et al*., "Uncertainty in seawater carbonate chemistry observations," *ESSD*, vol. 16, pp. 4573–4596, 2024. https://doi.org/10.5194/essd-16-4573-2024

[40] P. Friedlingstein *et al*., "Global Carbon Budget 2025," *ESSD*, vol. 18, pp. 3211–3299, 2026. https://doi.org/10.5194/essd-18-3211-2026

[41] A. Hogikyan and L. Resplandy, "Hydrological cycle amplification," *Biogeosciences*, vol. 21, pp. 4621–4639, 2024. https://doi.org/10.5194/bg-21-4621-2024

[42] R. G. J. Bellerby *et al*., "A new indicator for ocean acidification capacity," *Commun. Earth Environ.*, vol. 6, 2025. https://doi.org/10.1038/s43247-025-02380-4

[43] S. K. Lauvset *et al*., "GLODAPv2.2024 data product," *ESSD*, vol. 16, pp. 1381–1405, 2024. https://doi.org/10.5194/essd-16-1381-2024